

ENVIRONMENTAL RESEARCH CLIMATE



LETTER

Decreased northern hemisphere precipitation from consecutive CO₂ doublings is associated with significant AMOC weakening

OPEN ACCESS

RECEIVED
30 August 2024

REVISED
31 October 2024

ACCEPTED FOR PUBLICATION
14 November 2024

PUBLISHED
28 November 2024

Original content from this work may be used under the terms of the [Creative Commons Attribution 4.0 licence](#).

Any further distribution of this work must maintain attribution to the author(s) and the title of the work, journal citation and DOI.



X Zhang^{1,*} , D W Waugh² , I Mitevski³ , C Orbe^{4,5} and L M Polvani^{5,6}

¹ Department of Physics, University of Nevada, Reno, NV, United States of America

² Department of Earth and Planetary Sciences, Johns Hopkins University, Baltimore, MD, United States of America

³ Department of Geosciences, Princeton University, Princeton, NJ, United States of America

⁴ NASA Goddard Institute for Space Studies, New York, NY, United States of America

⁵ Department of Applied Physics and Applied Mathematics, Columbia University, New York, NY, United States of America

⁶ Lamont-Doherty Earth Observatory, Columbia University, Palisades, NY, United States of America

* Author to whom any correspondence should be addressed.

E-mail: xiyuez@unr.edu

Keywords: precipitation, abrupt CO₂ increase, AMOC, climate change

Supplementary material for this article is available [online](#)

Abstract

Previous studies found many climate properties such as northern hemisphere (NH) surface temperature and precipitation respond non-monotonically when CO₂ is increased from 1 × to 8 × CO₂ relative to pre-industrial levels. Here, we explore the robustness of the non-monotonicity in the NH precipitation response in 11 coupled climate models. Eight models show a decrease in NH precipitation under repeated CO₂ doubling, indicating that the non-monotonic response is a common but not universal result. Although common, the critical CO₂ level where the NH precipitation decrease first occurs differs widely across models, ranging from 2 × CO₂ to 8 × CO₂. These models also show a prominent weakening in the Atlantic meridional overturning circulation (AMOC) at the same critical CO₂ level, with the AMOC weakening leading the precipitation decrease. The sensitivities of NH precipitation and the AMOC to CO₂ doublings are positively correlated, especially when the AMOC weakens beyond 10 Sv. This suggests that the differences in models' AMOC response can explain their contrasting NH precipitation responses, where models with a large AMOC weakening have decreased NH precipitation. Regionally, this decrease in NH precipitation is the most prominent over the North Atlantic, Europe and the tropical Pacific. Our results suggest that special care must be taken with the use of pattern scaling to inform regional climate decision-making.

1. Introduction

In a recent study, Mitevski *et al* (2021, hereafter M21) found non-monotonic responses of a range of climate properties to CO₂ forcing in two fully coupled climate models. Specifically, they reported decreased northern hemisphere (NH) surface temperature, expanded Arctic sea ice extent, reduced NH precipitation, contracted subtropical dry zones, and a stronger NH Hadley cell with increasing CO₂ beyond some threshold value, in abrupt forcing simulations spanning 1–8 × CO₂. While this surprising behavior was found in both models, the threshold CO₂ concentration beyond which it occurred was different between the two models: it appeared between 2 × CO₂ and 3 × CO₂ for one model, but between 3 × CO₂ and 4 × CO₂ for the other model.

The mechanisms behind the non-monotonic response to CO₂ increase have also been explored. M21 found that the non-monotonicity is not present in the slab-ocean versions of the same models, clearly implicating a key role for ocean dynamics. Subsequent studies (Mitevski *et al* 2022, 2023, Orbe *et al* 2023) showed that such ocean dynamics are related to cooling over the North Atlantic (the North Atlantic warming hole, NAWH) and a concurrent weakening of the Atlantic meridional overturning circulation (AMOC). Multiple North Atlantic 'hosing' experiments have demonstrated that a weakened AMOC leads to the

Table 1. Model simulations used in this study. An x indicates the availability of output from coupled models. An ‘ s ’ indicates the availability of output from the slab-ocean configuration of the models. Critical CO₂ levels are indicated with $[c]$. Non-critical CO₂ level simulations used for composites on figures 3 and 5 are indicated with $[n]$.

Models	Pre-industrial (1×CO ₂)	2×CO ₂	4×CO ₂	8×CO ₂	Simulation references
GISS-E2.1	x, s	x, s	$x [c], s$	$x [n]$	Mitevski <i>et al</i> (2021)
CESM1	x, s	x, s	$x [c], s$	$x [n]$	Mitevski <i>et al</i> (2021)
CESM2	x	$x [c]$	$x [n]$		CMIP6/CFMIP-3
MRI-ESM2-0	x	$x [c]$	$x [n]$		CMIP6/CFMIP-3
CanESM5	x	x	x		CMIP6/CFMIP-3
HadCM3L	x	x	$x [n]$	$x [c]$	LongrunMIP
CESM104	x	x	x	x	LongrunMIP
MPIESM12	x	x	x	x	LongrunMIP
GISS-E2.2-OMA	x	$x [c]$	$x [n]$		CMIP6/CFMIP-3
GISS-E2.2-NINT	x	$x [n]$	$x [c]$		CMIP6/CFMIP-3
GISS-E2.2-LINOZ	x	$x [c]$	$x [n]$	x	Orbe <i>et al</i> (2024)

NAWH, decreased precipitation over the NH, and a southward shift of the ITCZ in coupled climate models (Zhang and Delworth 2005, Stouffer *et al* 2006, Jackson *et al* 2015, Liu *et al* 2020). The NAWH not only reduces local SSTs and the NH atmospheric moisture content (Jackson *et al* 2015), but also strengthens the meridional SST gradient and changes the cross-equatorial atmospheric heat transport (Moreno-Chamarro *et al* 2019), which explain the NH precipitation decrease.

This non-monotonic response has important implications when extrapolating results from 4×CO₂ simulations to other levels of CO₂ forcing (Chadwick and Good 2013). A particular application is the use of ‘pattern scaling’ that provides quantitative decision-relevant climate information on a regional scale over a range of scenarios (e.g. Lopez *et al* 2014). Furthermore, given the difference in CO₂ levels at which the non-monotonicity appears, it represents a plausible source of uncertainty in the model spread in response to 4×CO₂ forcing (e.g. Grise and Polvani 2016). However, there are several outstanding questions to be answered before examining how the non-monotonicity contributes to the inter-model spread of the atmospheric circulation response to 4×CO₂ forcing. First of all, it is not known whether the non-monotonicity occurs in all models, and how widely the critical CO₂ level varies across models. Furthermore, the robustness of the connection to the AMOC has only been recently explored in one climate model (Orbe *et al* 2023).

Here, we answer these questions by examining the response of NH precipitation, NAWH temperature, and the AMOC using models with abrupt 2×CO₂ and 4×CO₂ forcing simulations as part of the Coupled Model Intercomparison Project Phase 6 (CMIP6, Eyring *et al* 2016), as well as models with abrupt 2×CO₂, 4×CO₂, and 8×CO₂ forcing simulations available from LongrunMIP (Rugenstein *et al* 2019). We focus on NH precipitation as this field is available in all simulations (LongrunMIP has limited variables archived). Furthermore, a non-monotonic NH precipitation response is a good indicator of non-monotonic behavior in other circulation metrics as demonstrated by M21. In addition to NH averaged precipitation, we separately examine the precipitation response in the extratropical, subtropical, and deep tropical regions, to identify where the non-monotonicity is the most evident. We also analyze the spatial pattern of the precipitation response composited at critical and non-critical CO₂ levels.

2. Data and methods

We analyze the output from 11 coupled climate models for which there are 150 years of simulations with an abrupt doubling and quadrupling of CO₂ from pre-industrial levels (table 1, Zhang (2024)).

For six of these models, abrupt 8×CO₂ simulations are also available. This suite includes the two models (GISS-E2.1 and CESM1) analyzed in M21, five models (CESM2, MRI-ESM2-0, CanESM5, and GISS-E2.2-OMA and GISS-E2.2-NINT) from the Cloud Feedback Model Intermodal Comparison phase 3 (CFMIP-3, Webb *et al* 2017) with ocean overturning streamfunction output available, and three models (HadCM3L, CESM104, and MPIESM12) from LongrunMIP (Rugenstein *et al* 2019). We also include output from GISS-E2.2-LINOZ simulations (Orbe *et al* 2024), where the abrupt 2×CO₂ simulation is 140 years long. The CMIP6 archive includes two versions of GISS-E2.2 that differ in their treatment of atmospheric chemistry (the NINT version ‘physics version 1’ has no interactive chemistry and the OMA version ‘physics version 3’ has full tropospheric and stratospheric chemistry). GISS-E2.2-LINOZ has linearized stratospheric ozone chemistry but non-interactive tropospheric chemistry or aerosols. We also include the slab ocean

model (SOM) versions of the 60 year pre-industrial, abrupt $2\times\text{CO}_2$ and $4\times\text{CO}_2$ simulations from GISS-E2.1 and CESM1 (M21).

We calculate the averages of the last 50 years of the abrupt CO_2 simulations and 50 years of the pre-industrial simulations to represent the quasi-equilibrium states of each simulation in all models. We assess the significance of the equilibrium state for each simulation by showing the range of the 50 year mean values at 95% confidence interval using a Student's t-distribution. The variables of interest include precipitation (P), surface temperature (T_s), and the AMOC. We focus on the NH-averaged precipitation (P_{NH}) T_s averaged over the NAWH region ($45\text{--}65^\circ\text{N}$, $40\text{--}20^\circ\text{W}$) (T_{NAWH}), and the strength of the AMOC (ψ_{AMOC} , defined in M21 as the maximum Atlantic ocean overturning streamfunction between $30\text{--}55^\circ\text{N}$ and $800\text{--}2000\text{m}$). The last 30 years are averaged to represent the response for slab ocean simulations.

In a similar manner to Good *et al* (2016), we calculate the sensitivity of a quantity X to a CO_2 doubling by computing

$$\Delta_n X = X(n \times \text{CO}_2) - X\left(\frac{n}{2} \times \text{CO}_2\right),$$

where $X = (P_{\text{NH}}, T_{\text{NAWH}}, \psi_{\text{AMOC}})$ and $X(n \times \text{CO}_2)$ is X for the abrupt $n \times \text{CO}_2$ simulation. For example, $\Delta_4 P_{\text{NH}} = P_{\text{NH}}(4 \times \text{CO}_2) - P_{\text{NH}}(2 \times \text{CO}_2)$ is the change in NH-averaged precipitation between doubling and quadrupling CO_2 . We calculate $\Delta_n X$ for $n = 2, 4$, and 8 (when available). The significance of the sensitivity is assessed by comparing the two 50 year X samples using a two-sided Student's t-test at 95% confidence interval.

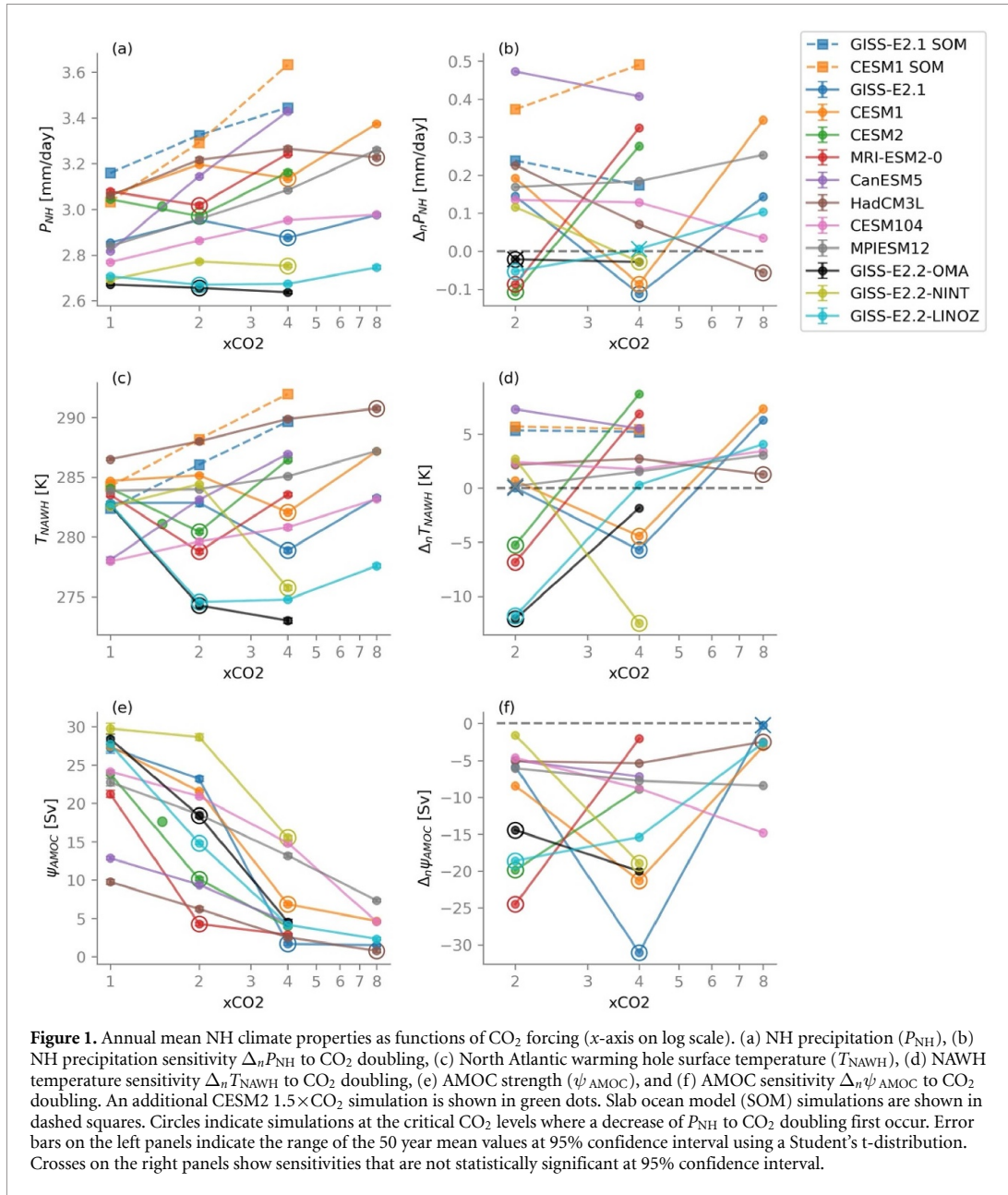
Assuming the CO_2 radiative forcing is a linear function of $\ln(n \times \text{CO}_2/1 \times \text{CO}_2)$ (e.g. Myhre *et al* 1998), if the response of X scales with radiative forcing then it will be also be linear with $\ln(n \times \text{CO}_2/1 \times \text{CO}_2)$. If so, $\Delta_n X$ will then be identical for all n , i.e. $\Delta_2 X = \Delta_4 X = \Delta_8 X$, and nonlinearity can be diagnosed by the difference in $\Delta_n X$ for different values of n . Here, our primary interest is the occurrence of non-monotonic responses to radiative forcing, which implies $\Delta_n X$ changes sign for increasing n . Because one expects an increase in global-mean P with increasing CO_2 (Pendergrass 2020), we focus here on the surprising occurrence of a decrease in P_{NH} under CO_2 doubling. In models where this occurs, we define the critical CO_2 level as the lowest value of n for which $\Delta_n P_{\text{NH}}$ is negative, i.e. if $\Delta_2 P_{\text{NH}} < 0$ for a model, then the critical CO_2 level for that model is $2 \times \text{CO}_2$. We average simulations at the critical CO_2 levels to produce multi-model mean time series of ψ_{AMOC} , P_{NH} , T_{NAWH} and maps of $\Delta_n T_{\text{NAWH}}$ and $\Delta_n P_{\text{NH}}$. For comparison, we also average simulations for adjacent non-critical CO_2 levels for each model (see table 1). We use the $2n \times \text{CO}_2$ simulation for the non-critical CO_2 levels, but if it is not available we use the $\frac{n}{2} \times \text{CO}_2$ simulation.

3. Results

3.1. NH precipitation, NAWH temperature, and AMOC responses

Among the models analyzed here, we have found a wide range of behavior in how P_{NH} responds to increased CO_2 (figure 1(a)), notably in the sign and magnitude of the change in P_{NH} for a doubling of CO_2 (figure 1(b)). Across all models and $n \times \text{CO}_2$, $\Delta_n P_{\text{NH}}$ varies from -0.12 to 0.47 mm d^{-1} , and 8 out of 11 models show $\Delta_n P_{\text{NH}} < 0$, for at least one n . Four models (CESM2, MRI-ESM2-0, GISS-E2.2-LINOZ, GISS-E2.2-OMA) show a decrease in P_{NH} first at $n = 2$ (although $\Delta_2 P_{\text{NH}}$ from GISS-E2.2-OMA is not statistically significant), three models (GISS-E2.1, CESM1, and GISS-E2.2-NINT) at $n = 4$, and one model (HadCM3L) at $n = 8$ (figure 1(b)). While three models (CanESM5, CESM104, and MPIESM12) show a monotonic increase of P_{NH} from $2 \times \text{CO}_2$ to $8 \times \text{CO}_2$, the response to CO_2 doubling is still nonlinear, i.e. $\Delta_n P_{\text{NH}}$ varies with n (figure 1(b)). This analysis, therefore, shows that while the M21 finding of a non-monotonic P_{NH} response is common, it is not universal. The non-monotonicity is also absent in slab ocean counterparts of GISS-E2.1 and CESM1 (figure 1(a)). Moreover, it shows that there is a large spread among models in the critical CO_2 level for a decrease in P_{NH} . M21 showed that a decrease in P_{NH} occurred between $2 \times \text{CO}_2$ and $3 \times \text{CO}_2$ for GISS-E2.1, and between $3 \times \text{CO}_2$ and $4 \times \text{CO}_2$ for CESM1 (in our analysis, which considers only $2x$ and $4 \times \text{CO}_2$, the critical CO_2 value is $n = 4$ for both models). However, figures 1(a) and (b) show that in other models this critical value can also be $2 \times \text{CO}_2$ or $8 \times \text{CO}_2$. Furthermore, an additional $1.5 \times \text{CO}_2$ simulation with CESM2 shows a decrease in P_{NH} from PI (figure 1(a)), so a decrease in P_{NH} can occur below $2 \times \text{CO}_2$.

M21 related the non-monotonic P_{NH} response to the non-monotonic response in NH-averaged T_s , and showed that it is only evident when the NAWH region is included. Consistent with this, we find a good correspondence between the T_{NAWH} and P_{NH} response in our suite of models (figures 1(c) and (d)). One can see a generally good agreement in the relative magnitude of $\Delta_n P_{\text{NH}}$ and $\Delta_n T_{\text{NAWH}}$, with models with large $\Delta_n P_{\text{NH}}$ also having large $\Delta_n T_{\text{NAWH}}$ (including the SOMs). More importantly, models that show a decrease in P_{NH} for CO_2 doubling also show a decrease in T_{NAWH} at the same critical n (figures 1(b) and (d)). HadCM3L



is the exception, but note that $\Delta_8 T_{NAWH}$ is close to zero for that model, i.e. there is little increase in T_{NAWH} from 4x to 8x CO₂, which is where P_{NH} decreases in that model.

Several recent studies have linked nonlinearity in the atmospheric and T_{NAWH} responses to differences in the AMOC response (e.g. Bellomo *et al* 2021, Mitevski *et al* 2021, 2022, 2023, Orbe *et al* 2023, Zhang *et al* 2023). We also find strong connections between the response in T_{NAWH} and P_{NH} and the response in ψ_{AMOC} . While all models show a ψ_{AMOC} decrease with increasing CO₂, the rate of the ψ_{AMOC} weakening varies greatly across models and with n (figure 1(e)). This variation is closely linked with variations in the P_{NH} and T_{NAWH} responses. Models with a small decrease in ψ_{AMOC} under CO₂ doubling show an increase in T_{NAWH} and P_{NH} . Models with a large decrease in ψ_{AMOC} show T_{NAWH} and P_{NH} decreases, indicating that a collapsed AMOC is associated with a decrease in T_{NAWH} and P_{NH} (figures 1(b), (d), and (f)). The $\Delta_n \psi_{AMOC}$ threshold for the different response is around -10 Sv, with $\Delta_n P_{NH} \leq 0$ and $\Delta_n T_{NAWH} \leq 0$ for $\Delta_n \psi_{AMOC} < -10$ Sv, but $\Delta_n P_{NH} > 0$ and $\Delta_n T_{NAWH} > 0$ for $\Delta_n \psi_{AMOC} > -10$ Sv. Again, HadCM3L is the exception, given that its pre-industrial ψ_{AMOC} is underestimated and around 10 Sv.

The interrelationships between $\Delta_n \psi_{AMOC}$, $\Delta_n T_{NAWH}$, and $\Delta_n P_{NH}$ are summarized in figure 2. A positive correlation between $\Delta_n \psi_{AMOC}$ and $\Delta_n P_{NH}$ is evident (with explained variance $r^2 = 0.48, p < 0.001$),

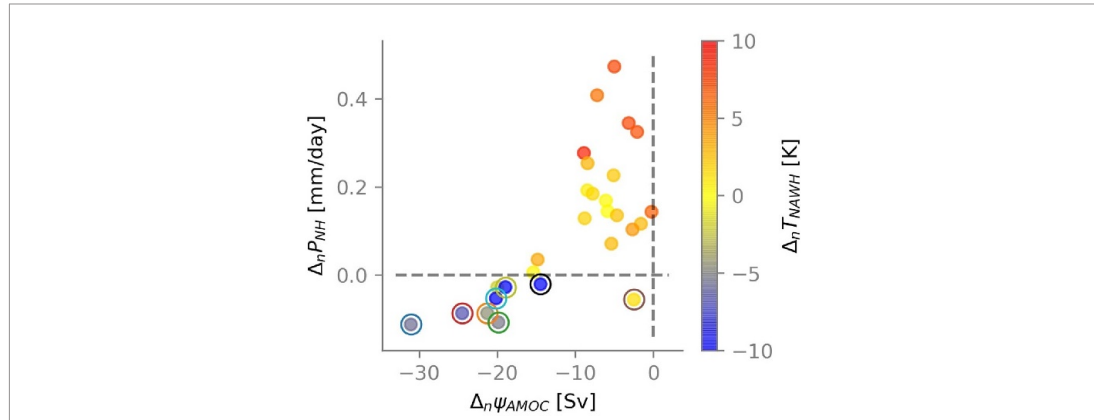


Figure 2. Scatter plots showing the relationship between AMOC sensitivity $\Delta_n\psi_{AMOC}$ and NH precipitation sensitivity Δ_nP_{NH} to CO_2 doubling. NAWH temperature sensitivity Δ_nT_{NAWH} is shown in colors. Circles indicate simulations at the critical CO_2 levels where a decrease of P_{NH} to CO_2 doubling first occurs (same as in figure 1).

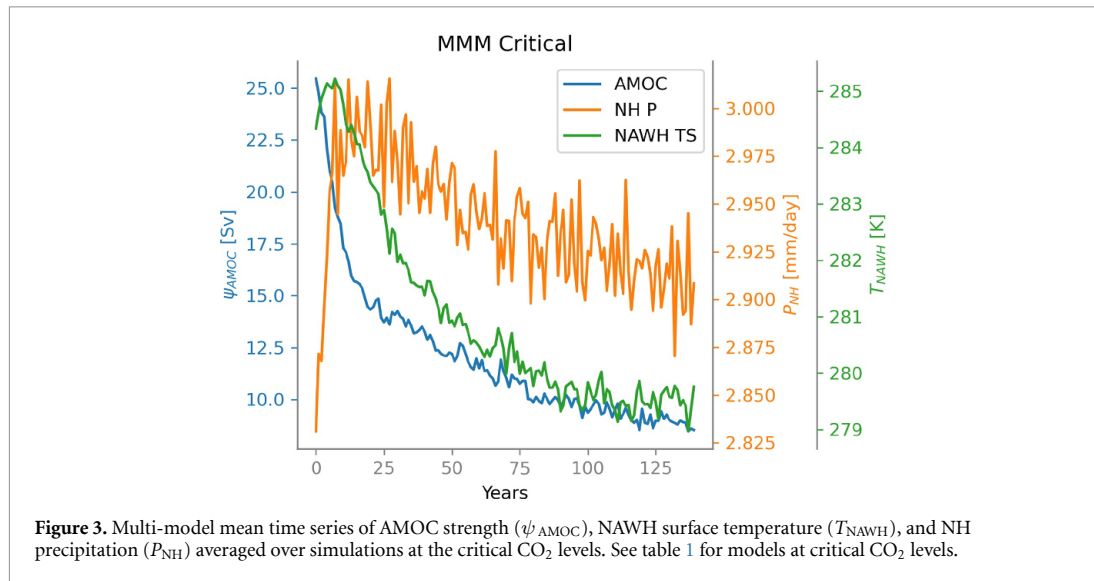


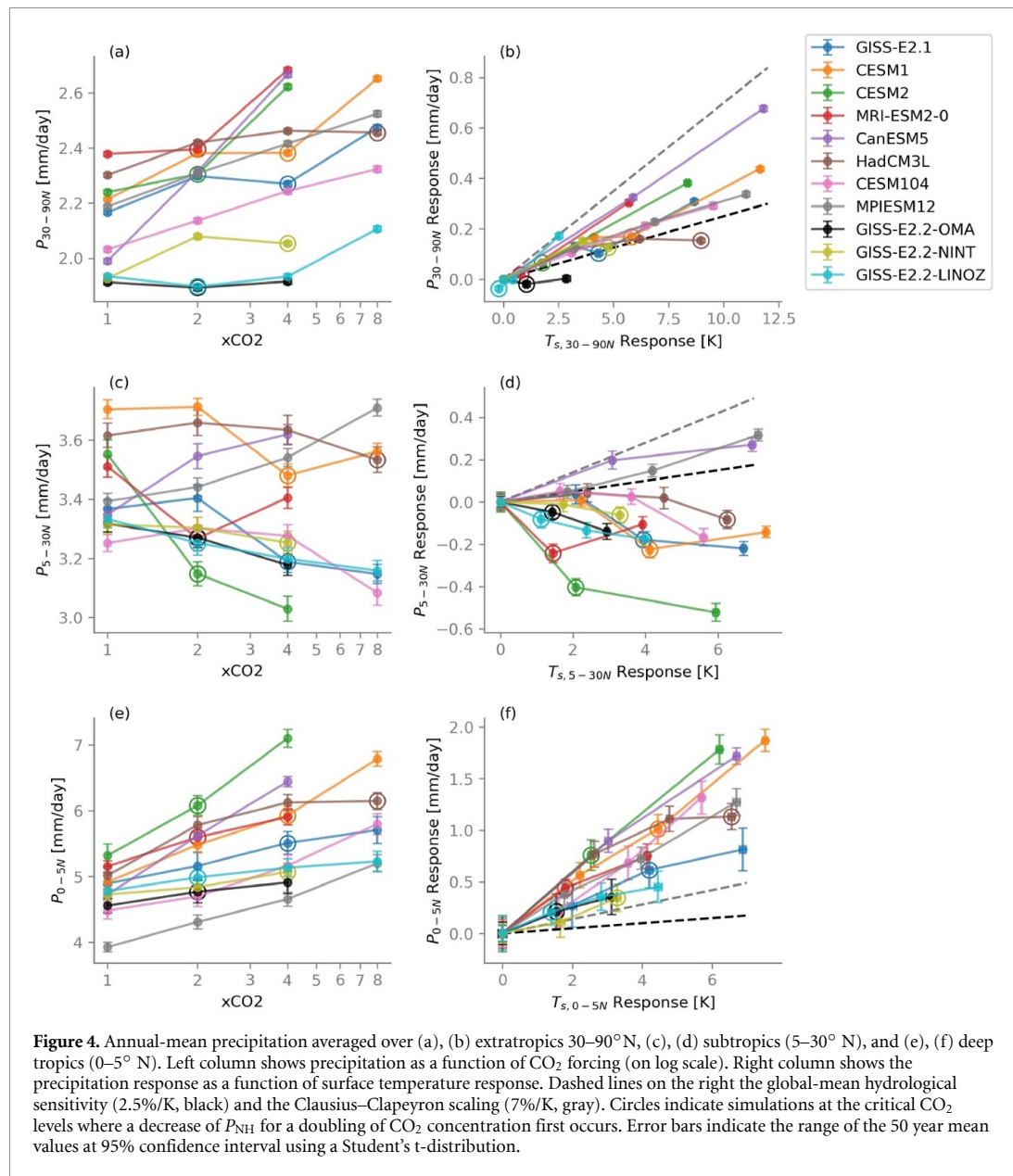
Figure 3. Multi-model mean time series of AMOC strength (ψ_{AMOC}), NAWH surface temperature (T_{NAWH}), and NH precipitation (P_{NH}) averaged over simulations at the critical CO_2 levels. See table 1 for models at critical CO_2 levels.

especially for $\Delta_n\psi_{AMOC} < -10$ Sv ($r^2 = 0.65, p < 0.01$). This suggests that a more negative $\Delta_n\psi_{AMOC}$ is associated with more negative Δ_nP_{NH} and Δ_nT_{NAWH} . For $\Delta_n\psi_{AMOC} > -10$ Sv, Δ_nP_{NH} shows little dependence on $\Delta_n\psi_{AMOC}$. However, larger Δ_nP_{NH} is associated with larger Δ_nT_{NAWH} . Therefore, when the decrease in ψ_{AMOC} is small, P_{NH} is largely influenced by other non-AMOC factors that can increase T_{NAWH} .

A closer look at the time series of ψ_{AMOC} , P_{NH} , and T_{NAWH} at the critical CO_2 levels offers insights into the evolution of these variables throughout the simulations (figure 3). Particularly, we find a lead-lag relationship between their responses to abrupt CO_2 increase. The AMOC strength decreases immediately after the abrupt CO_2 increase, while both P_{NH} and T_{NAWH} increase in the first 10 years. Then T_{NAWH} decreases drastically, reaching its pre-industrial value around Year 20, and continues to decrease until it stabilizes around Year 100. This cooling clearly lags the weakening of the AMOC. While P_{NH} displays large interannual variability, its decreasing trend is apparent after Year 20, which further lags the cooling of T_{NAWH} . The persistent decrease of P_{NH} after the first 20 years of the simulations results in a negative precipitation sensitivity Δ_nP_{NH} . While there are discernible inter-model differences in their ψ_{AMOC} , P_{NH} , and T_{NAWH} responses, there is a consistent picture of T_{NAWH} and P_{NH} decreases lagging behind the weakening of ψ_{AMOC} (figure S1). This suggests a critical role the AMOC weakening plays in driving the decrease in NAWH and NH precipitation.

3.2. Regional precipitation response

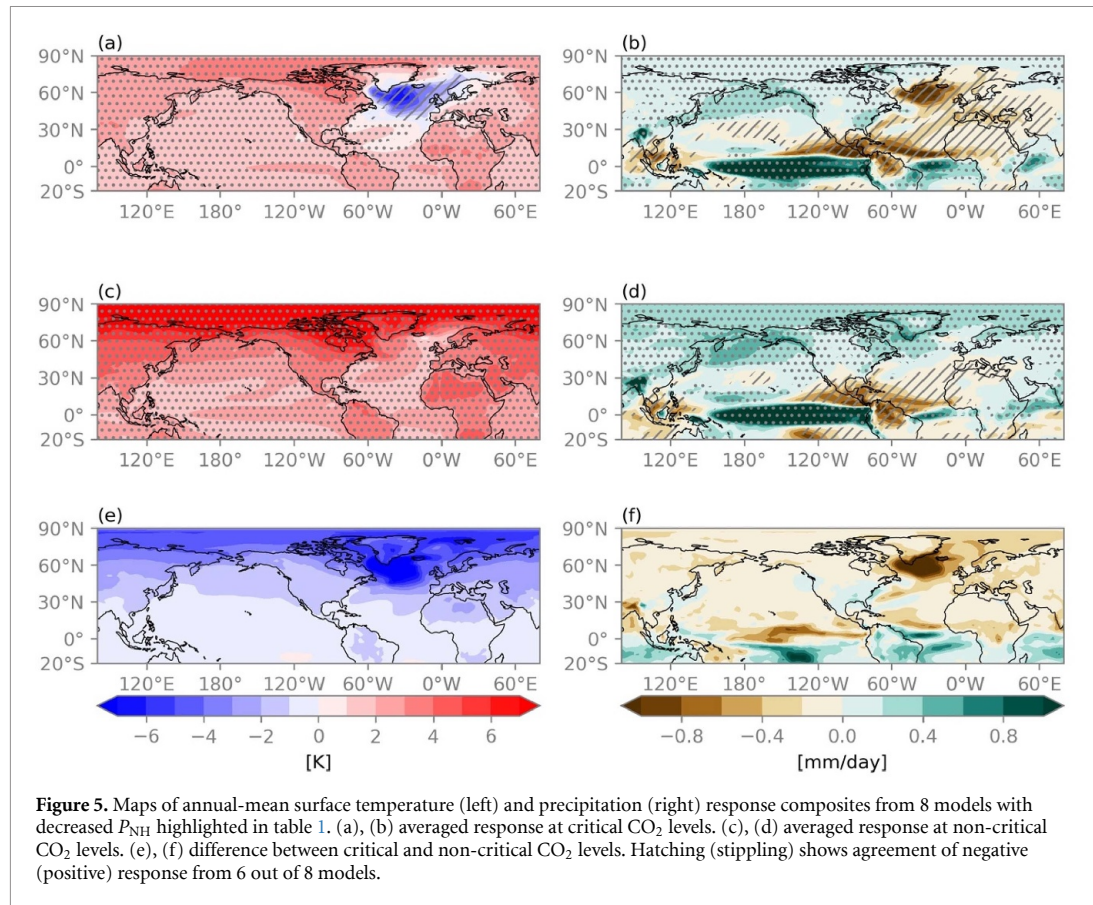
The above shows that in most models there exists a critical CO_2 level beyond which P_{NH} decreases upon CO_2 doubling, and that such decrease is related to a decrease in T_{NAWH} . Now we ask: Is this decrease occurring



across the entire NH, or is it limited to the cooling region around the NAWH? To explore this, we partition the P_{NH} response into the extratropical (30–90° N, P_{30-90N}), subtropical (5–30° N, P_{5-30N}), and deep-tropical (0–5° N, P_{0-5N}) regions (figure 4).

The response of P_{30-90N} to increasing CO₂ is similar to that of P_{NH} (figure 4(a)). Models that have a decrease in P_{NH} also show a decrease in P_{30-90N} at the same $n \times \text{CO}_2$, except for CESM2 and MRI-ESM2-0 where there is a slight increase, rather than decrease, in P_{30-90N} between $1 \times \text{CO}_2$ and $2 \times \text{CO}_2$. However, this increase is much less than the increase in P_{30-90N} between $2 \times \text{CO}_2$ and $4 \times \text{CO}_2$ for these two models, and their P_{30-90N} response is nonlinear. The response of P_{30-90N} largely scales with $T_{s,30-90N}$ response (figure 4(b)). The majority of the models have a regression slope between the global-mean hydrological sensitivity of 2.5%/K (black dashed line, Pendergrass 2020) and the Clausius–Clapeyron scaling of 7%/K (gray dashed line). Two models have deviations from this positive regression: GISS-E2.2-OMA shows invariant P_{30-90N} with $T_{s,30-90N}$ and HadCM3L at $8 \times \text{CO}_2$ shows a slight negative slope.

While the P_{30-90N} response is similar to that of P_{NH} , it is notable that the decrease in P_{30-90N} at the critical CO₂ level is smaller in magnitude, indicating that precipitation must also decrease at lower latitudes. These decreases occur within the subtropics, where nearly all models show a general decrease in P_{5-30N} with increasing CO₂ (figure 4(c)). This decrease is also manifested in negative regression slopes with $T_{s,5-30N}$



response across most models (figure 4(d)). The decrease in P_{5-30N} is most prominent at the critical CO_2 levels (circles in figure 4(c)), which suggests that subtropical drying under increased CO_2 is further exaggerated when the AMOC is significantly weakened. It is notable that the P_{5-30N} decrease at this forcing is much larger in magnitude than that for P_{30-90N} . In other words, most the decrease in P_{NH} is coming from the subtropics and not the extratropics.

As we move to the deep tropics, P_{0-5N} increases monotonically with CO_2 in all models (figure 4(e)). The response of P_{0-5N} scales positively with $T_{s,0-5N}$ response at slopes much steeper than the Clausius–Clapeyron scaling (figure 4(f)). Simulations at the critical CO_2 level are not distinguishable from other simulations, except for HadCM3L at $8\times CO_2$. This suggests that P_{0-5N} is dominated by the response to CO_2 increase and less influenced by changes in ψ_{AMOC} .

The latitudinal difference in P response motivates us to look into the spatial patterns in more detail. We investigate composite maps of $\Delta_n T_s$ and $\Delta_n P$ averaged over 8 models that show a decrease in P_{NH} at their critical CO_2 levels (figures 5(a) and (b)), and compare them to their adjacent non-critical CO_2 average (figures 5(c) and (d), see Table for adjacent non-critical CO_2 values for each model). Their differences quantify the spatial pattern of the nonlinear T_s and P responses (figures 5(e) and (f)).

Models at critical CO_2 levels show strong cooling in the NAWH (figure 5(a)) and have smaller Arctic amplification than models at non-critical CO_2 levels (figure 5(c)). The difference between models at critical and non-critical levels is characterized by polar-amplified cooling that is the strongest over the NAWH and the Arctic Ocean (figure 5(e)). Northern Africa and Eurasia also show weaker $\Delta_n T_s$ increase at critical CO_2 levels (compare 5(a) and 5(c)).

The pattern of $\Delta_n P$ from the non-critical CO_2 composite shows the typical ‘wet gets wetter, dry gets dryer’ pattern, whereas at critical CO_2 levels the models show more negative $\Delta_n P$ across the NH (figures 5(b) and (d)). Specifically, the NAWH, the tropical Pacific, the subtropical Atlantic, and much of Europe and North Africa show a stronger decrease in P . The model agreement on having negative $\Delta_n P$ over NAWH,

Europe, and Northern Africa is also much higher at the critical CO₂ levels (figure 5(b)). This highlights the inhomogeneous character of the precipitation response nonlinearity to CO₂ forcing, especially in the Atlantic basin, which is consistent with what is seen in T_s (figure 5(e)). In the Pacific, although the P nonlinearity is weak in the extratropics, we find a dipole response in the tropical Pacific that is consistent with a southward ITCZ shift (figure 5(f)). These findings suggest far-reaching impacts on P outside of the North Atlantic from a collapsed AMOC.

4. Summary and discussions

We have tested the robustness of the non-monotonic P_{NH} response to increased CO₂ reported for two climate models by Mitevski *et al* (2021). Out of 11 couple climate models examined, 8 show a decrease of P_{NH} in response to a doubling of CO₂ concentration. This indicates the non-monotonic response is a common, but not universal, result. Although common, the critical CO₂ level beyond which the P_{NH} decrease occurs differs widely across models, ranging from $2\times\text{CO}_2$ to $8\times\text{CO}_2$ (with an additional simulation in one model showing a decrease for only $1.5\times\text{CO}_2$).

A decrease in T_{NAWH} in response to a doubling of CO₂ is also found in these models, at the same critical CO₂ as for P_{NH} . Furthermore, at this critical CO₂ level we find a collapse of the AMOC, with ψ_{AMOC} weakening by more than 10 Sv for a doubling of CO₂. This suggests that the differences in models' AMOC response can explain their contrasting T_{NAWH} and P_{NH} responses. Models with a large weakening of AMOC for a doubling of CO₂ tend to have cooler NH surface temperature and decreased NH precipitation.

The decrease in NH precipitation at the critical CO₂ occurs primarily over the Atlantic, and extends to Europe and North Africa, but is not confined to the NAWH region. In addition to a P decrease in mid-latitudes, we find a decrease in the subtropics, consistent with a southward shift of the northern edge of the ITCZ. This is consistent with a dynamical strengthening of the NH Hadley cell due to AMOC weakening (Zhang and Delworth 2005, Liu *et al* 2017, Orihuela-Pinto *et al* 2022, Orbe *et al* 2023). While the spatial pattern of simulated precipitation response to climate change is to generally enhance the climatological precipitation pattern (e.g. Held and Soden 2006), we here highlight the key role of the AMOC response in shaping the global pattern of the precipitation response.

The correlation between the P_{NH} and the ψ_{AMOC} responses to CO₂ doubling suggests that the non-monotonic P_{NH} response to CO₂ increase can be largely attributed to the nonlinear AMOC response. While the NAWH can also form due to atmospheric processes or North Atlantic gyre circulation changes (Keil *et al* 2020, He *et al* 2022, Li *et al* 2022), its presence is a major fingerprint of the AMOC weakening (Menary and Wood 2018). Our time series analysis supports this hypothesis, given that the AMOC weakening leads the formation of NAWH and P_{NH} decrease. This is consistent with Bellomo *et al* (2021), who found climate models with larger AMOC decline for $4\times\text{CO}_2$ simulations have cooler NH surface temperature and decreased NH precipitation. This conclusion is further supported by multiple North Atlantic 'hosing' studies which have analyzed experiments that artificially weaken the AMOC in coupled climate models, and have found precipitation decreases over the NH, particularly in the NAWH region and Europe (Bellomo *et al* 2023, Stouffer *et al* 2006, Jackson *et al* 2015, Liu *et al* 2020, Orihuela-Pinto *et al* 2022). A weaker AMOC also induces a southward shift of the ITCZ (Zhang and Delworth 2005, Jackson *et al* 2015, Moreno-Chamarro *et al* 2019), resulting in a dipole response of the tropical Atlantic precipitation (Stouffer *et al* 2006, Liu *et al* 2017, 2020). Although a detailed discussion of the mechanisms underlying the AMOC-induced precipitation response is beyond the scope of this paper, these earlier studies have noted the roles of thermodynamics, energetics, and storm track dynamics. While we have here focused mainly on NH precipitation, we expect other aspects of the NH response to show similar non-monotonic behavior (Mitevski *et al* 2021). For example, nonlinear response in the AMOC has shown to be associated with a nonlinear midlatitude jet response (Bellomo *et al* 2021, Orbe *et al* 2023, Zhang *et al* 2023). Subtropical and tropical precipitation is also tightly connected to the Hadley Cell strength and edge location. As demonstrated in M21, both the NH Hadley cell strength and the dry zone edge show non-monotonic behavior similar to P_{NH} . In future work, we plan to explore the monotonicity of other aspects of the climate system response, as well as their connection to the AMOC.

Data availability statement

CMIP6 data can be accessed at <https://esgf-node.llnl.gov/search/cmip6/>. The Python script used for data processing and plotting are available upon request to the corresponding author.

The data that support the findings of this study are openly available at the following URL/DOI: <https://doi.org/10.5281/zenodo.14188021> (Zhang 2024).

Acknowledgment

We thank the two anonymous reviewers for their constructive feedback. We thank the LongRunMIP organizers for providing access to their datasets. This work was partially supported by the National Science Foundation Awards 2335761 and 1914569. We would like to acknowledge high-performance computing support from the Derecho system (doi:10.5065/qx9a-pg09) provided by the NSF National Center for Atmospheric Research (NCAR), sponsored by the National Science Foundation.

ORCID iDs

X Zhang  <https://orcid.org/0000-0002-6031-7830>
D W Waugh  <https://orcid.org/0000-0001-7692-2798>
I Mitevski  <https://orcid.org/0000-0001-9172-3236>
C Orbe  <https://orcid.org/0000-0002-5344-3599>
L M Polvani  <https://orcid.org/0000-0003-4775-8110>

References

- Bellomo K, Angeloni M, Corti S and von Hardenberg J 2021 Future climate change shaped by inter-model differences in Atlantic meridional overturning circulation response *Nat. Commun.* **12** 1–10
- Bellomo K, Meccia V L, D'Agostino R, Fabiano F, Larson S M, von Hardenberg J and Corti S 2023 Impacts of a weakened AMOC on precipitation over the Euro-Atlantic region in the EC-Earth3 climate model *Clim. Dyn.* **61** 3397–416
- Chadwick R and Good P 2013 Understanding nonlinear tropical precipitation responses to CO₂ forcing *Geophys. Res. Lett.* **40** 4911–5
- Eyring V, Bony S, Meehl G A, Senior C A, Stevens B, Stouffer R J and Taylor K E 2016 Overview of the coupled model intercomparison project phase 6 (CMIP6) experimental design and organization *Geosci. Model Dev.* **9** 1937–58
- Good P, Andrews T, Chadwick R, Dufresne J L, Gregory J M, Lowe J A, Schaller N and Shiogama H 2016 nonlinMIP contribution to CMIP6: model intercomparison project for non-linear mechanisms: physical basis, experimental design and analysis principles (v1.0) *Geosci. Model Dev.* **9** 4019–28
- Grise K M and Polvani L M 2016 Is climate sensitivity related to dynamical sensitivity? *J. Geophys. Res.* **121** 5159–76
- He C, Clement A C, Cane M A, Murphy L N, Klavans J M and Fenske T M 2022 A North Atlantic warming hole without ocean circulation *Geophys. Res. Lett.* **49** e2022GL100420
- Held I M and Soden B J 2006 Robust responses of the hydrological cycle to global warming *J. Clim.* **19** 5686–99
- Jackson L C, Kahana R, Graham T, Ringer M A, Woollings T, Mecking J V and Wood R A 2015 Global and European climate impacts of a slowdown of the AMOC in a high resolution GCM *Clim. Dyn.* **45** 3299–316
- Keil P, Mauritsen T, Jungclaus J, Hedemann C, Olonscheck D and Ghosh R 2020 Multiple drivers of the North Atlantic warming hole *Nat. Clim. Change* **10** 667–71
- Li L, Lozier M S and Li F 2022 Century-long cooling trend in subpolar North Atlantic forced by atmosphere: an alternative explanation *Clim. Dyn.* **58** 2249–67
- Liu W, Fedorov A V, Xie SP and Hu S 2020 Climate impacts of a weakened Atlantic meridional overturning circulation in a warming climate *Sci. Adv.* **6** eaaz4876
- Liu W, Xie SP, Liu Z and Zhu J 2017 Overlooked possibility of a collapsed Atlantic meridional overturning circulation in warming climate *Sci. Adv.* **3** e1601666
- Lopez A, Suckling E B and Smith L A 2014 Robustness of pattern scaled climate change scenarios for adaptation decision support *Clim. Change* **122** 555–66
- Menary M B and Wood R A 2018 An anatomy of the projected North Atlantic warming hole in CMIP5 models *Clim. Dyn.* **50** 3063–80
- Mitevski I, Dong Y, Polvani L M, Rugenstein M and Orbe C 2023 Non-monotonic feedback dependence under abrupt CO₂ forcing due to a North Atlantic pattern effect *Geophys. Res. Lett.* **50** e2023GL103617
- Mitevski I, Orbe C, Chemke R, Nazarenko L and Polvani L M 2021 Non-monotonic response of the climate system to abrupt CO₂ Forcing *Geophys. Res. Lett.* **48** e2020GL090861
- Mitevski I, Polvani L M and Orbe C 2022 Asymmetric warming/cooling response to CO₂ increase/decrease mainly due to non-logarithmic forcing, not feedbacks *Geophys. Res. Lett.* **49** e2021GL097133
- Moreno-Chamarro E, Marshall J and Delworth T L 2019 Linking ITCZ migrations to the AMOC and North Atlantic/Pacific SST decadal variability *J. Clim.* **33** 893–905
- Myhre G, Highwood E J, Shine K P and Stordal F 1998 New estimates of radiative forcing due to well mixed greenhouse gases *Geophys. Res. Lett.* **25** 2715–8
- Orbe C, Rind D, Miller R L, Nazarenko L, Romanou A, Jonas J, Russell G, Kelley M and Schmidt G 2023 Atmospheric response to a collapse of the North Atlantic circulation under a mid-range future climate scenario: a regime shift in northern hemisphere dynamics *J. Clim.* **36** 6669–93
- Orbe C, Rind D, Waugh D W, Jonas J, Zhang X, Chiodo G, Nazarenko L and Schmidt G A 2024 Coupled Stratospheric Ozone and Atlantic Meridional Overturning Circulation Feedbacks on the northern hemisphere Midlatitude Jet Response to 4xCO₂ *J. Clim.* **37** 2897–917
- Orihuela-Pinto B, England M H and Taschetto A S 2022 Interbasin and interhemispheric impacts of a collapsed Atlantic overturning circulation *Nat. Clim. Change* **12** 558–65
- Pendergrass A G 2020 The global-mean precipitation response to CO₂-induced warming in CMIP6 models *Geophys. Res. Lett.* **47** e2020GL089964
- Rugenstein M *et al* 2019 LongRunMIP: motivation and design for a large collection of millennial-length AOGCM simulations *Bull. Am. Meteorol. Soc.* **100** 2551–70

- Stouffer R J *et al* 2006 Investigating the causes of the response of the thermohaline circulation to past and future climate changes *J. Clim.* **19** 1365–87
- Webb M J *et al* 2017 The cloud feedback model intercomparison project (CFMIP) contribution to CMIP6 *Geosci. Model Dev.* **10** 359–84
- Zhang R and Delworth T L 2005 Simulated tropical response to a substantial weakening of the Atlantic thermohaline circulation *J. Clim.* **18** 1853–60
- Zhang X 2024 Dataset for 'Decreased northern hemisphere precipitation from consecutive CO₂ doublings is associated with significant AMOC weakening' [Data set] *Environmental Research: Climate* (Zenodo) (<https://doi.org/10.5281/zenodo.14188021>)
- Zhang X, Waugh D W and Orbe C 2023 dependence of northern hemisphere tropospheric transport on the midlatitude jet under abrupt CO₂ increase *J. Geophys. Res.* **128** e2022JD038454